

Performance Analysis of Hybrid Solid Oxide Fuel Cell - Gas Turbine Power System

Abdulrazzak Akroot^a, Abdullah Nadeesh^b

^aDepartment of Mechanical Engineering, Karabuk University, Turkey

^bDepartment of Chemical Engineering, Konya Technical University, Turkey

ABSTRACT

Energy and exergy analyses are introduced to a zero-dimensional hybrid system of solid oxide fuel cell - gas turbine, for steady-state operation. The effects of two important SOFC parameters (operating pressure and current density) on varying conditions are examined. According to the obtained results, a decrease in SOFC current density improved the system performance (electrical efficiencies and exergy efficiencies) due, primarily, to the reduction in Ohmic losses, which results in a higher stack voltage. As system pressure increases, net electrical power, electrical system efficiency, and electrical system exergy increase to a peak and then decrease. The main exergy destructions occur in the combustion chamber and the gas turbine.

KEYWORDS: Solid oxide fuel cell, Hybrid system, Current density, System pressure, Exergy destruction, Efficiency.

Date of Submission: 30-09-2020

Date of Acceptance: 13-10-2020

I. INTRODUCTION

Solid oxide fuel cells (SOFC) are electrochemical devices that convert the free chemical energy of hydrogen from fuel directly into electrical energy with high efficiency and resulting emits the waste heat and water. SOFC is very promising because it is a high-energy conversion efficiency of up to 80%, and it is very appropriate for a broad application prospect of power generation systems. Besides, the properties of high efficiency, it has a high-quality exhaust heat and low emission, which allows the creating a hybrid power system with a gas turbine (GT) or micro gas turbine (MGT). The SOFC electrochemical reactions take place at relatively high temperatures compared to the other types of fuel cells[1–7].

Many investigators have studied theoretical simulation and analysis of the possible configuration of hybrid power plants. Park et al [8] simulated the design of a pressurized SOFC hybrid system using a fixed gas turbine. Bavarsad[9] investigated an internal reforming SOFC/GT hybrid system to study the effect of different parameters such as fuel and air flow rates, temperature, and pressure on the performance of the system. Ishak et al [10] presented the integration of direct ammonia solid oxide fuel cell with a gas turbine in a new combined cooling, heating, and power cycle. Akroot[11] studied the impact of various SOFC operation temperatures on the performance of the hybrid system. Zabihiyan and Fung [12] investigated the effects of the inlet fuel type and composition on the performance of hybrid solid oxide fuel cell (SOFC) and gas turbine (GT) model. Zhang et al [13] established a novel model of the SOFC–GT hybrid system with internal reforming to determine the optimal rate of fuel flowing into SOFC and calculate the maximum efficiency of the hybrid system. Mehrpooya et al [14] introduced a two-dimensional finite difference model of hybrid solid oxide fuel cell-gas turbine power plants. The results showed that the voltage and electric power increase as pressure and temperature rise. Lv et al [15] studied the effect of key operating parameters such as F/A ratio, S/C ratio, and rotational speed on the SOFC hybrid system

The aim of the current study is, first, energy and exergy analysis of a SOFC/GT integrated power plant, in which energy balance and exergy balance are done for each component of the hybrid system individually to identify the inlet and outlet condition of the corresponding streams and then assessing the performance of the system. For model simulation, a Matlab[®] code is used to calculate thermodynamic properties for all parts of the power plant and analysis the performance of the hybrid system. Also, the effect of various parameters, such as current density, and SOFC operation temperature are studied on the system performance.

SYSTEM MODELING AND ASSUMPTIONS

The plant layout is shown in Figure 1. The system consists of a SOFC stack, a combustion chamber, a gas turbine, a water pump, mixers, compressors, and heat exchangers. The operation of the system can be summarized as follows: The fuel and air entering the system are pressurized separately by the fuel and air compressors, to the fuel cell operating pressure before being preheated in the heat exchangers by the exhaust

gases. Liquid water is compressed by the pump to the fuel cell operating pressure and then preheated in the heat exchanger (HE3) to convert it to water vapor and then it is supplied to the mixer to mixed with methane. The methane gas must be reacted with steam to converts to H₂, H₂O, CO, and CO₂ in the reforming and shifting reactions at the inlet of the anode. The electrochemical reaction occurs in the SOFC stack to produces electricity, thermal energy, and water. The unburned fuel and excess air react in the combustion chamber to increase the temperature of the exhaust gas. The high thermal energy of the exhaust gases is expanded through a gas turbine to generate mechanical power, which in turn is converted into additional electric power.

AC: AIR COMPRESSOR
FC: Fuel compressor
M: Mixer
GT: Gas turbine
HE: Heat exchanger
CC: Combustion chamber

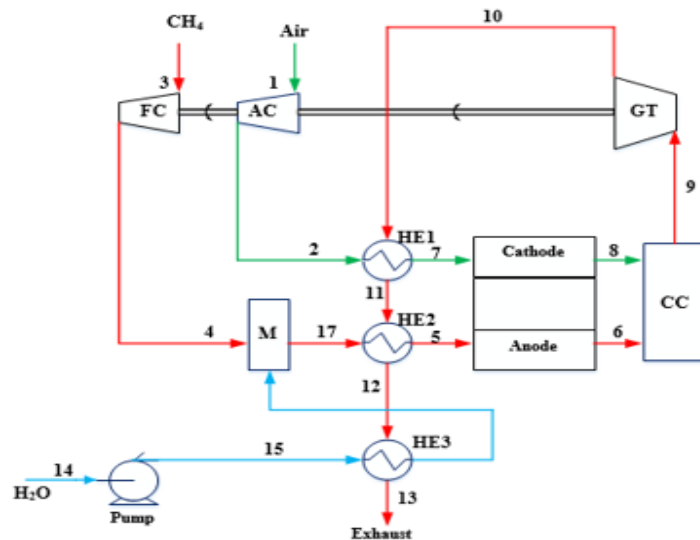


Figure 1. Diagram of the SOFC /GT hybrid system

The developed model for SOFC is made on the following assumptions [3,16] with the system modeling parameters listed in Table 1:

- The system performs under steady-state conditions.
- Air, methane, and water enter the fuel cell with the same temperature.
- Air enters the SOFC with molar fractions of 21% for O₂ and 79% for N₂.
- The methane is completely reformed to hydrogen before taking part in the electrochemical reaction.
- The stream temperatures at the exits of the SOFC cathode and the anode are the same.
- There is no heat interaction with the environment.
- Only hydrogen is electrochemically reacted. CO is converted to CO₂ and H₂ by water–gas shift reaction.

Table 1. The SOFC stack parameters

Parameter	Value
Specific resistivity of the anode	$95 \times 10^6 \exp\left(\frac{11150}{T_{sofc}}\right)^{-1}$
Specific resistivity of cathode	$42 \times 10^6 \exp\left(\frac{11200}{T_{sofc}}\right)^{-1}$
Specific resistivity of the electrolyte	$3.34 \times 10^4 \exp\left(\frac{10300}{T_{sofc}}\right)^{-1}$
Specific resistivity of interconnection	$9.3 \times 10^6 \exp\left(\frac{11100}{T_{sofc}}\right)^{-1}$
Active surface area	0.01 (m ²)
Thickness of anode	500 (μm)
Thickness of cathode	50 (μm)
Thickness of electrolyte	10 (μm)
Thickness of interconnect	0.3×10^{-2} (m)
Exchange current density of the anode	6500(A/m ²)
Exchange current density of the cathode	2500 (A/m ²)
Baseline current density	6000 (A/m ²)
Effective gaseous diffusivity through the anode	0.2×10^{-4} (m ² /s)
Effective gaseous diffusivity through the cathode	0.05×10^{-4} (m ² /s)
Stack pressure drop	2 %

Fuel utilization factor	0.85(-)
Number of cells	667

FUEL CELL MODEL

The solid oxide fuel cell was simulated via a zero-dimensional steady-state model built-in Matlab®. The SOFC design was based on anode-supported, planar configuration, and consists of 667 cells. The electrolyte, anode, and cathode were composed of yttria-stabilized zirconia (YSZ), nickel-doped yttria-stabilized zirconia (Ni-YSZ), and lanthanum strontium magnetite (LSM), respectively.

The cell voltage E_{cell} , is calculated by subtracting the activation, ohmic, and concentration overpotentials from the Nernst potential (i.e., open circuit voltage), E_{ocv} :

$$E_{cell} = E_{ocv} - \eta_{act} - \eta_{ohm} - \eta_{con} \tag{1}$$

$$E_{ocv}(T, P_i) = -\frac{\Delta G}{nF} + \frac{RT}{2F} \ln \left[\frac{P_{H_2} \cdot P_{O_2}^{1/2}}{P_{H_2O}} \right] \tag{2}$$

$$\eta_{act} = \frac{RT_{sofc}}{F} \sinh^{-1} \left(\frac{i}{2i_{oa}} \right) + \frac{RT_{sofc}}{F} \sinh^{-1} \left(\frac{i}{2i_{oc}} \right) \tag{3}$$

$$i = 2i_o \sinh \left(\frac{n_e F \eta_{act}}{2RT_{sofc}} \right) \tag{4}$$

$$\eta_{ohm} = i(\rho_a \delta_a + \rho_c \delta_c + \rho_e \delta_e + \rho_i \delta_i) \tag{5}$$

$$\eta_{con, a/c} = -\frac{RT_{sofc}}{n_e F} \ln \left(1 - \frac{i}{i_{L,a/c}} \right) \tag{6}$$

The stack voltage is simply the cell voltage multiplied by the number of cells:

$$V_{stack} = E_{cell} \cdot n_{cell} \tag{7}$$

The stack power (P_{SOFC}) can be calculated as:

$$P_{SOFC} = i \cdot A_{cell} \cdot E_{cell} \cdot n_{cell} = i \cdot A_{cell} \cdot V_{stack} \tag{8}$$

ENERGY AND EXERGY ANALYSIS OF SYSTEM

Energy balance for a hybrid system component at steady-state and neglecting changes in kinetic and potential energy can be written as:

$$\dot{Q} + \dot{W} = \sum_i n_i \bar{h}_i + \sum_e n_e \bar{h}_e \tag{9}$$

where \dot{Q} , \dot{W} , and \bar{h}_i represent heat transfer rate, work transfer rate, and molar enthalpy, respectively. The energy balance applied to determine the energy efficiency of the system is given in Table 3.

Table 3. Performance criteria

Parameter	Value
Input energy	$\dot{Q}_{in} = \dot{n}_{CH_4} \cdot LHV_{CH_4}$
Input exergy	$\dot{E}_{in} = \dot{n}_{CH_4} \cdot \bar{e}_f^{kim}$
Net electrical power of the system	$P_{Net} = P_{SOFC} + W_{GT} - W_{AC} - W_{FC} - W_{PUMP}$
SOFC efficiency	$\eta_{sofc} = P_{SOFC} / \dot{Q}_{in} \cdot 100$
Overall electrical efficiency	$\eta_{overall} = P_{Net} / \dot{Q}_{in} \cdot 100$
exergy efficiency of SOFC	$\psi_{sofc} = P_{SOFC} / \dot{E}_{in} \cdot 100$
overall electrical exergy efficiency	$\psi_{electricity} = P_{Net} / \dot{E}_{in} \cdot 100$

The specific exergy is the total of the chemical exergy and physical exergy. The chemical exergy change is linked with chemical processes while the physical exergy is obtained from mechanical and thermal processes. Physical and chemical exergy for each node of the model should be determined as follow [17]:

$$\dot{E}x_j^f = \sum_i \dot{n}_i [\bar{h}_i - \bar{h}_{o,i} - T_o (\bar{s}_i - \bar{s}_{o,i})] \tag{10}$$

$$\dot{E}x_j^c = \sum_i \dot{n}_i [x_i \bar{e}_i^{kim} + \bar{R} T_o x_i \ln(x_i)] \tag{11}$$

where $\dot{E}x_j^f$ and $\dot{E}x_j^c$ are the physical and chemical exergy, T_o is the ambient temperature, \bar{s}_i is the specific molar entropy, x is the molar fraction of the gas i at each node, and \bar{e}_i^{kim} is the standard chemical exergy of gases, as shown in table 4. The total exergy for each node in the system is calculated as follow:

$$\dot{E}x_j = \dot{E}x_j^f + \dot{E}x_j^c \tag{12}$$

The exergy rate balance of a control volume at steady state can be expressed as:

$$\dot{I} = \sum_j (1 - T_o/T_j) \dot{Q} + \dot{W}_{CV} + \sum_j \dot{E}x_i + \sum_e \dot{E}x_e \tag{13}$$

Table 4. Standard chemical exergy of gases [18]

Gases	Standard Chemical Exergy (kJ/mole)
CH ₄	831.6
H ₂	236.1
O ₂	3.97
N ₂	0.72
CO	275.
CO ₂	19.87
H ₂ O(<i>g</i>)	9.5

MODEL VALIDATION

The polarization curve of the SOFC model used in this study has been compared with one model from the literature. In the differentiation, the operating conditions (temperature and pressure) are assumed to be the same as the ones assumed in the case research presented from Ranjbar et al.[17], which are 1000 K and 1.19 atm respectively. As presented in Figure 2, the polarization curve of this work matches very well with the preceding work results, and the divergence between these results does not exceed 1%.

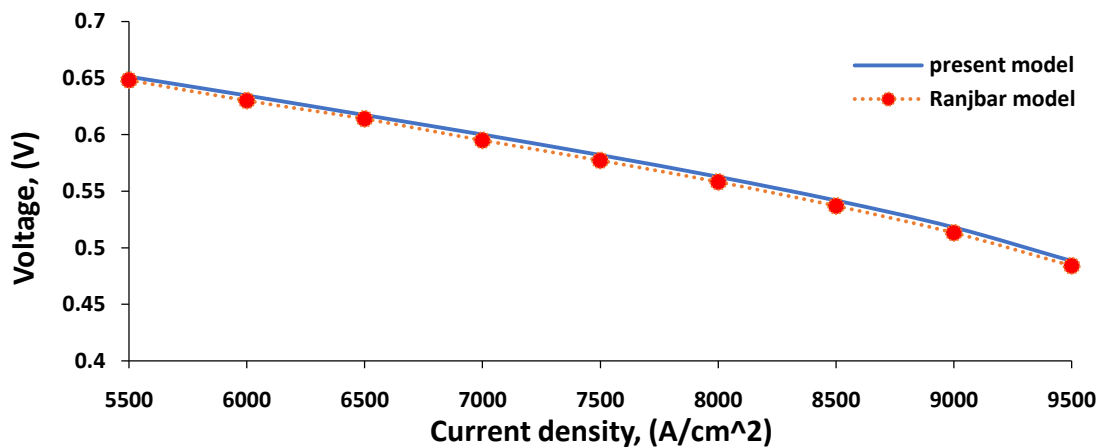


Figure 2. Differentiation between the polarization curve obtained from this work and the data from a preceding work by Ranjbar et al,[17].

II. RESULTS AND DISCUSSION

The model under discussion is simulated at full-load steady-state performance based on fixed setting parameters as a reference case. The compressor efficiency 85%, pump efficiency 85%, afterburner combustion efficiency 99%, heat exchangers pressure drop 3%, the effectiveness of heat exchangers 80%, afterburner pressure drop 5,% S/C ratio 2.0, and fuel utilization 85%. Results of the base case simulation at current density 6000A/cm² are shown in Table 2. The rate of exergy destruction in cycle components is shown in Figure 3.

Table 2. Base case simulation results

Cell voltage	Electrical efficiency	Stack power	Net power	η_I	η_{II}
0.7382	59.17%	28.95	33.28	68.02	65.61

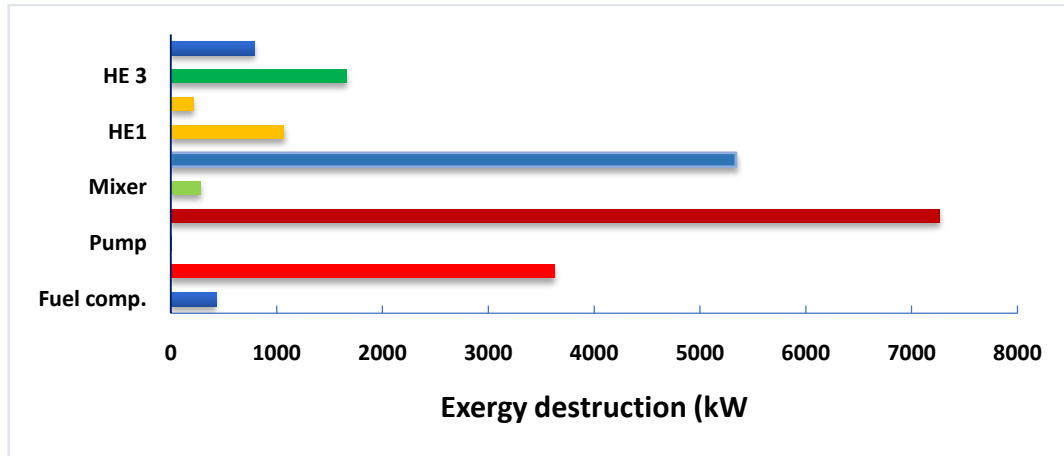


Figure 3. Exergy destruction in various components of the existing system

Current density: The SOFC current density is a significant parameter for evaluating system performance. Figures 4–6 indicate the effect of current density on the voltage, power output, energy efficiency, and exergy efficiency. Figure 4 shows the impact of SOFC current density on the cell voltage, stack power density, and power output. As can be seen, increment the current density decreases the cell voltage due to the increases in the total voltage loss. Cell voltage decreases from 0.8206 to 0.6671 (about 18.7%). It is also seen from the figure that the stack power and the power output from the hybrid system directly proportional to the SOFC current density. The SOFC stack power increases from 16.15 to 39.14 kW (about 58%) and the system stack power increases from 18.29 to 45.7 kW (about 60%), thus denoting that the hybrid system gives more power at high current density.

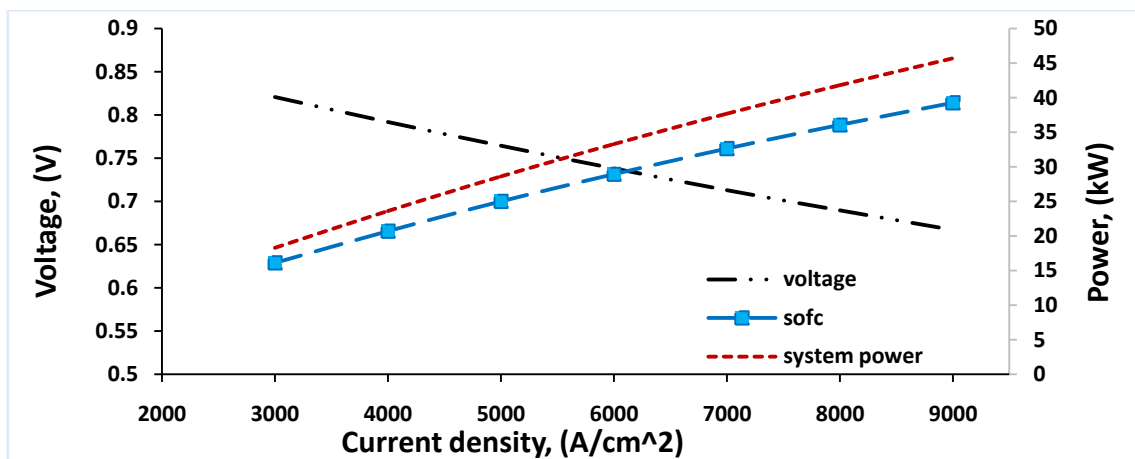


Figure 4. Fuel cell voltage, stack power density, and power output as a function of SOFC current density

A SOFC- GT hybrid system requires the use of some components such as compressors and pumps that require power input. As a result, the auxiliary power consumed by these devices must be subtracted from the overall gross power generated by the hybrid system to calculate the total power output from the system.

Figure 5 reveals the effect of SOFC current density on the power of the main components of the hybrid system. The molar flow rates of air and fuel directly proportional to the SOFC current density. Therefore, the power consumed by the air and fuel compressors increases with the increase in SOFC current density. It is possible to see from this figure that the electrical power consumed by the air compressor is growing faster than the rate of electrical power consumed by the fuel compressor due to elevating the airflow rate through the air compressor.

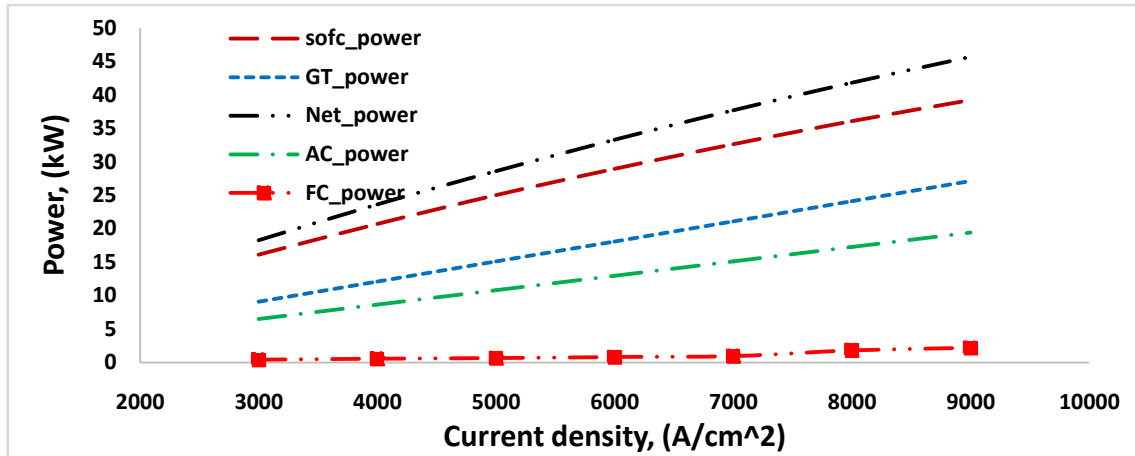


Figure 5. Power of the main components as a function of SOFC current density

Figure 6 shows the influence of SOFC current density on the hybrid system performance. The curves in these figures show the SOFC electrical efficiency, SOFC exergy efficiency, system electrical efficiency, and system exergy efficiency for different values of current densities. It is viewed from the curves that the increase of SOFC current density decreases SOFC efficiencies and system efficiencies because of the raised in the molar flow rate of fuel and it causes an increase in the inlet fuel energy and exergy. Increasing inlet energy and exergy hurt the system efficiencies and fuel cell efficiencies.

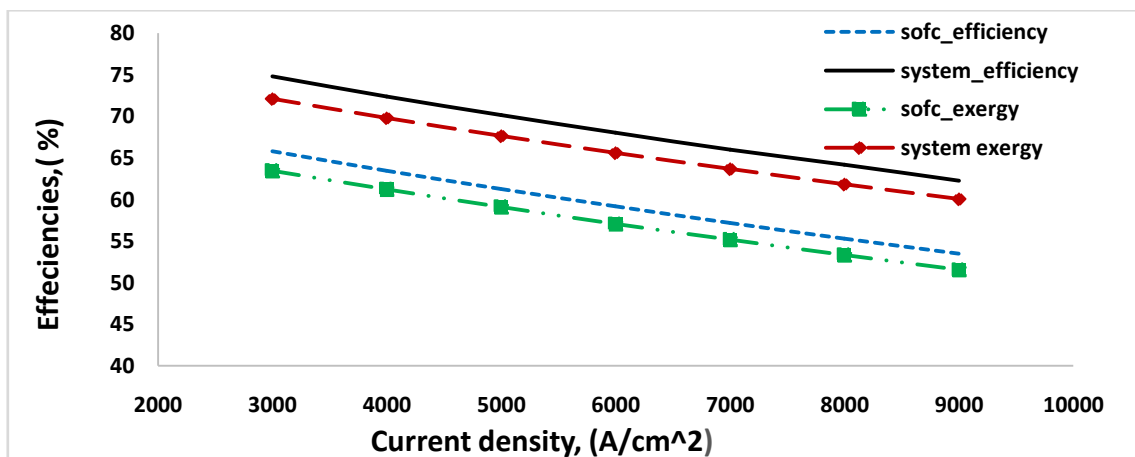


Figure 6 Hybrid system efficiencies as a function of SOFC current density

Operation pressure: Air and CH₄ pressure are important parameters in system performance. Figures 7-9 display the impact of operating pressure on voltage, efficiency, and power output. Figure 7 showed that the effect of system pressure on the voltage and power output from the hybrid system. It is seen from the figure that an increase in the operating pressure gives rise to an increment in the stack power due to the reduction in the voltage losses. It is indicated from the figure that when system pressure increases from 4 bar to 12 bar, the SOFC stack power increases from 28.49 to 29.66 kW (about 4%).

The results also showed that the net electrical power increases with increasing system pressure reaches a maximum and then decreases as the system pressure further increases. When the system pressure dramatically increases, the auxiliary power consumed by the air compressor raises that lead to a decrease in the net electrical power. A considerable elevate in the net output power should be observed, with a maximum of 33.5 kW at 8 bar.

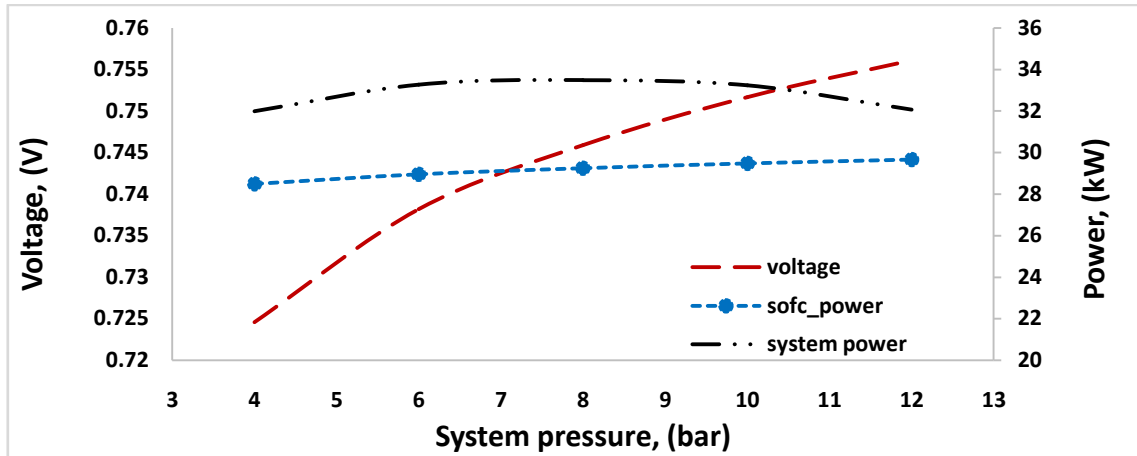


Figure 7. Fuel cell voltage and stack power density as a function of SOFC current density for two different models

Figure 8 shows the influence of system pressure on the power of the main components of the hybrid system. As shown in the figure, the power consumed by the auxiliary components (pump, air, and fuel compressors) increases with the increase in the system operating pressure. It also can be seen from the figure that the increment of the system pressure leads to a rise in the turbine inlet pressure, resulting in promote of gas turbine power output.

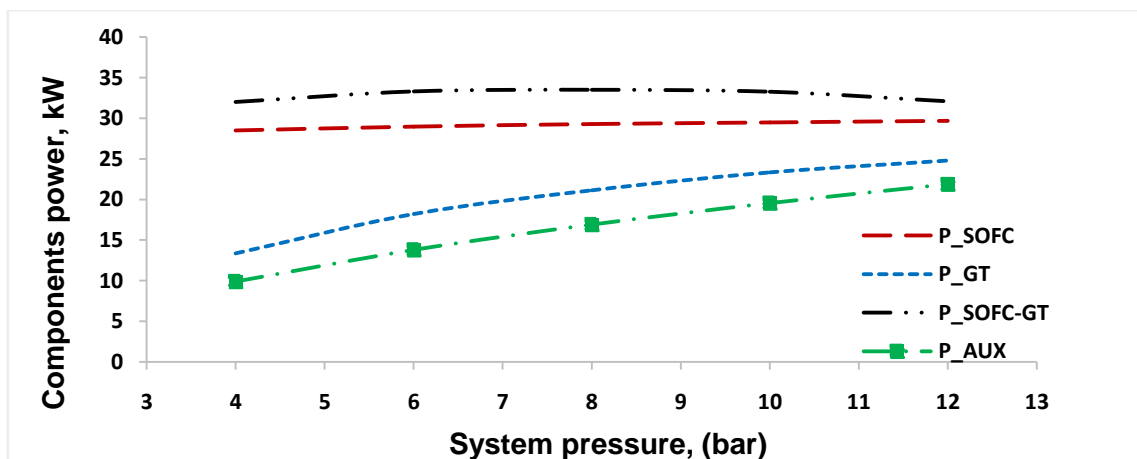


Figure 8. Power of the main components as a function of system pressure for two different models

Figure 9 shows the relationship between system pressure and system performance. The SOFC voltage and its power output elevate when the system pressure increases, resulting in an enhanced in the SOFC efficiencies as seen in the figure. The figure also presented that the increase of the system pressure leads to rising in the turbine inlet pressure, resulting in an increment in the power output from the gas turbine and lifting in the power consumption in the air and fuel compressors. When the system pressure increases, the system efficiencies increase reaches a maximum and then begins to decline as the system pressure further increases.

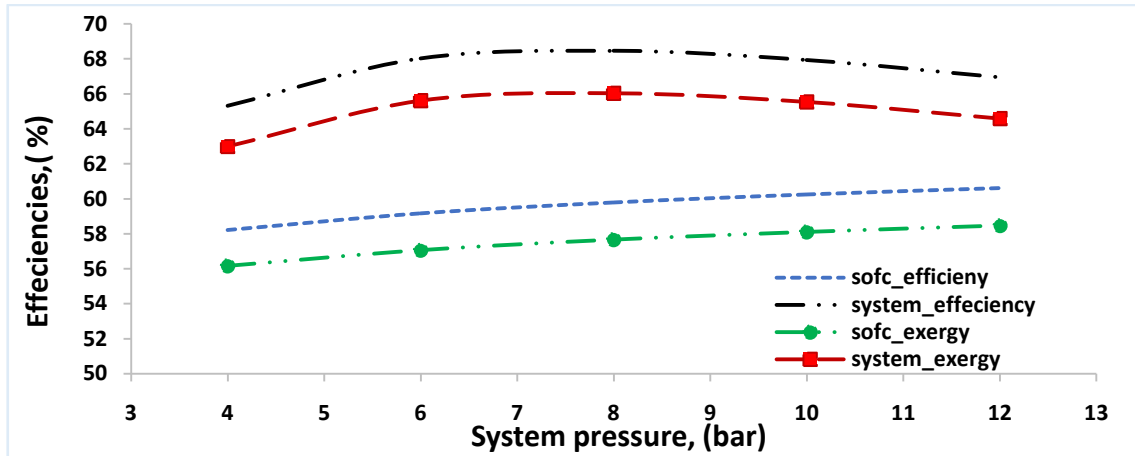


Figure 9 Hybrid system efficiencies as a function of system operating pressure

III. CONCLUSIONS

In this study, energy and exergy analysis of a zero-dimensional steady-state SOFC-GT hybrid system was developed in Matlab®. The hybrid system model was used to investigate the impacts of some various operating parameters such as system pressure, SOFC current density on the power output, and the performance of a selected hybrid system. Several remarkable conclusions can be drawn from the results of this study:

- ❖ Increasing the operating pressure of the hybrid system increases net electrical power, electrical system efficiency, and electrical system exergy until reaches a maximum and then falls as the operating pressure further increases because of the increment in the auxiliary power consumed by the compressors.
- ❖ Operating the hybrid system at a high pressure caused an increase in the cell voltage, resulting in an improved on the stack power, efficiency, and exergy of SOFC.
- ❖ The decrease of SOFC current density improved the system performance (electrical efficiencies and exergy efficiencies) due, primarily, to the reduction in Ohmic losses, which results in a higher stack voltage.
- ❖ The main exergy destructions occur in the combustion chamber and the gas turbine.

NOMENCLATURE

- A_{cell} Cell area, (cm²)
 - E_{OCV} Fuel cell voltage at standard conditions, (V)
 - $\dot{E}x_j^f$ Physical exergy, (kJ)
 - $\dot{E}x_j^c$ Chemical exergy, (kJ)
 - \bar{e}_i^{km} Standard chemical exergy of gases, (kJ/mol)
 - F Faraday constant, (C/mol)
 - ΔG Change in molar Gibbs free energy, (J/mol)
 - LHV Lower heating value, (kJ/mol)
 - T_o Ambient temperature,
 - \bar{s}_i Specific molar entropy, (J/mol K)
 - \bar{h} Molar enthalpy, (J/mol)
 - i Current density in Ampere, (A. cm²)
 - n Number of moles of electrons transferred
 - P_i Partial pressure of gas, (Pa)
 - \dot{Q} Heat transfer rate across the boundary of the system, (kW)
 - \dot{W} Work transfer rate, (kW)
 - P Power, (kW)
 - T Absolute temperature, (K)
 - R Universal gas constant, (J/mol K)
 - v_{stack} Stack voltage, (V)
- Greek Letters**
- δ Thickness, (cm)
 - η Energy efficiency
 - Ψ Exergy efficiency
 - ρ Electrical resistivity, ($\Omega^{-1} \text{ cm}^{-1}$)
 - i_o Exchange current density, (A cm⁻²)

Acronyms

CCCombustion chamber

FCFuel compressor

GTGas turbine

MMixer

SOFCSolid oxide fuel cell

HE Heat exchanger

REFERENCE

- [1]. J. Larminie, A. Dicks, Fuel cell systems explained: Second edition, 2013. <https://doi.org/10.1002/9781118878330>.
- [2]. S.C. Singhal, K. Kendall, High-temperature Solid Oxide Fuel Cells: Fundamentals, Design and Applications, 2003. <https://doi.org/10.1016/B978-1-85617-387-2.X5016-8>.
- [3]. A. Akroot, L. Namli, H. Ozcan, Compared Thermal Modeling of Anode- and Electrolyte-Supported SOFC-Gas Turbine Hybrid Systems, J. Electrochem. Energy Convers. Storage. (2021). <https://doi.org/10.1115/1.4046185>.
- [4]. X.Y. Zhou, A. Pramuanjaroenkij, S. Kakaç, A Review on Miniaturization of Solid Oxide Fuel Cell Power Sources-II: From System to Material, in: 2008. https://doi.org/10.1007/978-1-4020-8295-5_22.
- [5]. N.Q. Minh, Solid oxide fuel cell technology - Features and applications, Solid State Ionics. (2004). <https://doi.org/10.1016/j.ssi.2004.07.042>.
- [6]. A. Elleuch, K. Halouani, Y. Li, Bio-methanol fueled intermediate temperature solid oxide fuel cell: A future solution as component in auxiliary power unit for eco-transportation, Mater. Des. (2016). <https://doi.org/10.1016/j.matdes.2016.02.060>.
- [7]. D. Papurello, A. Lanzini, L. Tognana, S. Silvestri, M. Santarelli, Waste to energy: Exploitation of biogas from organic waste in a 500 Wel solid oxide fuel cell (SOFC) stack, Energy. (2015). <https://doi.org/10.1016/j.energy.2015.03.093>.
- [8]. S.K. Park, K.S. Oh, T.S. Kim, Analysis of the design of a pressurized SOFC hybrid system using a fixed gas turbine design, J. Power Sources. (2007). <https://doi.org/10.1016/j.jpowsour.2007.03.067>.
- [9]. P.G. Bavarsad, Energy and exergy analysis of internal reforming solid oxide fuel cell-gas turbine hybrid system, Int. J. Hydrogen Energy. (2007). <https://doi.org/10.1016/j.ijhydene.2007.08.004>.
- [10]. F. Ishak, I. Dincer, C. Zamfirescu, Energy and exergy analyses of direct ammonia solid oxide fuel cell integrated with gas turbine power cycle, J. Power Sources. (2012). <https://doi.org/10.1016/j.jpowsour.2012.03.083>.
- [11]. A. Akroot, Effect of Operating Temperatures on the Performance of a SOFCGT Hybrid System, Int. J. Trend Sci. Res. Dev. Volume-3 (2019) 1512–1515. <https://doi.org/10.31142/ijtsrd23412>.
- [12]. F. Zabihian, A.S. Fung, Performance analysis of hybrid solid oxide fuel cell and gas turbine cycle: Application of alternative fuels, Energy Convers. Manag. (2013). <https://doi.org/10.1016/j.enconman.2013.08.005>.
- [13]. X. Zhang, Y. Wang, T. Liu, J. Chen, Theoretical basis and performance optimization analysis of a solid oxide fuel cell-gas turbine hybrid system with fuel reforming, Energy Convers. Manag. (2014). <https://doi.org/10.1016/j.enconman.2014.06.068>.
- [14]. M. Mehrpooya, S. Akbarpour, A. Vatani, M.A. Rosen, Modeling and optimum design of hybrid solid oxide fuel cell-gas turbine power plants, Int. J. Hydrogen Energy. (2014). <https://doi.org/10.1016/j.ijhydene.2014.10.077>.
- [15]. X. Lv, C. Lu, Y. Wang, Y. Weng, Effect of operating parameters on a hybrid system of intermediate-temperature solid oxide fuel cell and gas turbine, Energy. (2015). <https://doi.org/10.1016/j.energy.2015.07.100>.
- [16]. C.O. Colpan, I. Dincer, F. Hamdullahpur, Thermodynamic modeling of direct internal reforming solid oxide fuel cells operating with syngas, Int. J. Hydrogen Energy. (2007). <https://doi.org/10.1016/j.ijhydene.2006.10.059>.
- [17]. F. Ranjbar, A. Chitsaz, S.M.S. Mahmoudi, S. Khalilarya, M.A. Rosen, Energy and exergy assessments of a novel trigeneration system based on a solid oxide fuel cell, Energy Convers. Manag. (2014). <https://doi.org/10.1016/j.enconman.2014.07.014>.
- [18]. The Exergy Method of Thermal Plant Analysis, 1985. <https://doi.org/10.1016/c2013-0-00894-8>.

Abdulrazzak Akroot, et. al. "Performance Analysis of Hybrid Solid Oxide Fuel Cell - Gas Turbine Power System" *The International Journal of Engineering and Science (IJES)*, 9(9), (2020): pp. 43-51.